Numerical Simulation on the Growth of Hot Gas Spots Produced by a Spark Discharge

K.Momose, G.Komatsu and Y.Hosokawa
Department of Mechanical Engineering
Himeji Institute of Technology
2167 Shosha, Himeji 671-22
Japan
A.Ueda and T.Iwata
Mitsubishi Electric Corporation

ABSTRACT

The formation process of hot gas spots produced by composite sparks in the vicinity of spark gap has beeen investigated by a numerical simulation. In the simulation the full Navier-Stokes equations were solved by the MacCormack scheme with heat generation supplied by composite sparks which are including the capacitive discharge component and the inductive discharge one. The calculated results indicate that, the strong convection field is formmed in the early stage in the vicinity of the spark gap due to the large pressure difference caused by the capacitive discharge, and the thermal energy released by the subsequent inductive discharge is transported into the gas by the convection and formed hot gas spots.

INTRODUCTION

It is important to know thermal convection phenomena of hot gas spots produced by composite sparks for improving of the ignition ability of the spark, emissions and the fuel consumption. In general, composite sparks compose of capacitive-discharge component and the subsequent inductive-discharge one, which have very short discharge time and comparatively long one respectively. It is well known that, giving only the inductive component for combustible mixtures is not enough to ignite, the some capacitive component needs for it. However, the reason is not established yet because of complexity of the ignition phenomena, although systematic works have been carried out(1-5). It seems to be necessary the theoretical and fundamental research.

The purpose of this study is to learn basically about how the capacitive discharge and the inductive discharge during composite sparks affect the growth and decay of hot gas spots. We are regarding the growth of hot gas spots after a spark discharge as a purelly thermal problem, and aiming to investigate the growth of hot gas(air) spots, its decay, pressure and gas velocity in the atmosphere without gas flow.

The spark discharge considered in this simulation was treated as a heat generation of air by discharge energy with finite volume. The calculation domain is consisted of spark discharge gap, surface of electrode, symmetric boundaries and pseudo-far-field boundaries. In this simulation, the time-dependent compressible Navier-Stoke equations were solved with the unsteady heat generation term including the capacitive-discharge component and the inductive-discharge one.

FORMULATION OF THE PROBLEM

Governing Equations

The conservation law form of the time-dependent compressible Navier-Stokes equations with heat generation term in cylindrical coordinate can be written as

$$\frac{\partial U}{\partial t} + \frac{1}{r}\frac{\partial}{\partial r}(rF) + \frac{\partial G}{\partial z} = S \qquad (1)$$

where r and z are the radial and axial coordinates, and

$$U = \begin{bmatrix} \rho \\ \rho u \\ \rho v \\ e \end{bmatrix},$$

$$F = \begin{bmatrix} \rho u \\ \rho u^2 + p - \tau_{rr} \\ \rho uv + \tau_{rz} \\ (e + p - \tau_{rr})u - \tau_{zr}v + q_r \end{bmatrix},$$

$$G = \begin{bmatrix} \rho v \\ \rho vu - \tau_{zr} \\ \rho v^2 + p - \tau_{zz} \\ (e + p - \tau_{zz})v - \tau_{rz}u + q_z \end{bmatrix},$$

$$S = \begin{bmatrix} 0 \\ (p - \tau_{\theta\theta})/r \\ 0 \\ Q \end{bmatrix} \qquad (2)$$

where Q is the heat generation per unit

volume supplied by spark discharge energy, and plays a main role to generate a flow field and a thermal field.
The stress tensors τ for a Newtonian fluid are written as

$$\tau_{rr} = 2\mu\frac{\partial u}{\partial r} + \lambda\left[\frac{1}{r}\frac{\partial}{\partial r}(ru) + \frac{\partial v}{\partial z}\right],$$

$$\tau_{zz} = 2\mu\frac{\partial v}{\partial z} + \lambda\left[\frac{1}{r}\frac{\partial}{\partial r}(ru) + \frac{\partial v}{\partial z}\right],$$

$$\tau_{rz} = \tau_{zr} = \mu\left(\frac{\partial v}{\partial r} + \frac{\partial u}{\partial z}\right),$$

$$\tau_{\theta\theta} = 2\mu\frac{u}{r} + \lambda\left[\frac{1}{r}\frac{\partial}{\partial r}(ru) + \frac{\partial v}{\partial z}\right]. \quad (3)$$

When Fourier's law of heat conduction is assumed, the heat flux vector can be expressed as

$$q_r = -\kappa\frac{\partial T}{\partial r}, \qquad q_z = -\kappa\frac{\partial T}{\partial z}. \quad (4)$$

Finally, the system is closed using the perfect gas equation of state and the thermodynamic relation as below

$$p = \rho R T = (\gamma - 1)[e - 0.5\rho(u^2 + v^2)] \quad (5)$$

where R is the gas constant and γ is the ratio of specific heats.
In this simulation, the air is assumed as a fluid, and the coefficients of viscosity is calculated using Sutherland's equation and Stokes hypothesis

$$\mu = \frac{1.5\times10^{-6}T^{3/2}}{T + 123.6}, \qquad \lambda = -\mu\frac{2}{3} \quad \text{Pa·s} \quad (6)$$

and the following relation has been used as a coefficient of heat conductivity.

$$\kappa = 7.56\times10^{-5}T + 3.517\times10^{-3} \quad \text{W/mK} \quad (7)$$

Computational Procedure

The computational domain, which is bounded by pseudo-far-field for discrete computation, is shown in Fig. 1. By taking advantage of symmetry with respect to both the axis of electrodes and the center plane

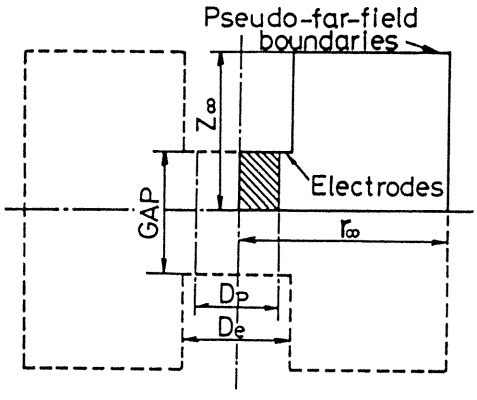

Fig. 1 Computational domain

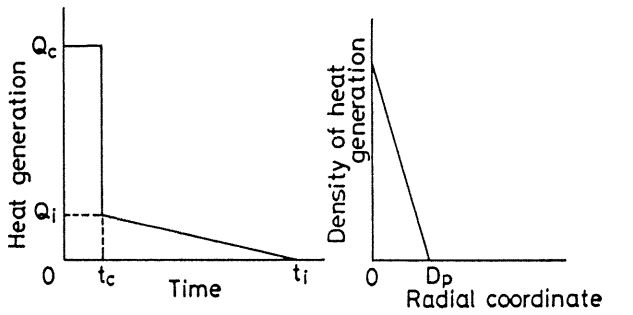

(a) Time pattern (b) Spatial pattern

Fig. 2 Discharge patterns for simulation

between them, only the region bounded by solid line was used as a computational domain. In all simulations, both the diameter of electrodes and the gap between them were set to 1 mm and pseudo-far-field baundaries were placed at 2 mm in r-direction and 1.5 mm in z-direction.

In this study, it is assumed that the discharge energy is transformed into a heat generation of air in the hatched area, and the diameter which is corresponds to that of discharge plasma is set to 0.6 mm in all simulations. The time and spatial pattern of heat generation used in the simulations are shown in Figs. 2(a) and 2(b). The capacitive and inductive discharge energy correspond to the heat generation Qc and Qi respectively.

The numerical calculations were performed by the explicit MacCormack scheme(6). As the initial conditions, it is assumed that the calculation domain is filled with air of room temperature and atomospheric pressure. As the boundary condition on the surface of electrodes, an adiabatic wall condition is used.

RESULTS AND DISCUSSION

In this study, the effects of three different types of discharge on the growth of hot gas spots are investigated by numerical simulation. The discharge conditions is listed in table 1. Type A is modeled as a capacitive discharge, so the density of discharge energy is large and discharge period is very short. On the other hand, type B has comparatively small density of energy and long discharge period, so this type is modeled as a inductive discharge. The total energy of type A and type B, however, are the same. Type C is the composite discharge in which type B combined with type A, and this type is modeled as a real ignition discharge.

Table 1 Discharge conditions

type	Q_c (W)	t_c (μs)	Q_i (W)	t_i (μs)
A	1000	0.1	0	0
B	0	0	20	10
C	1000	0.1	20	10

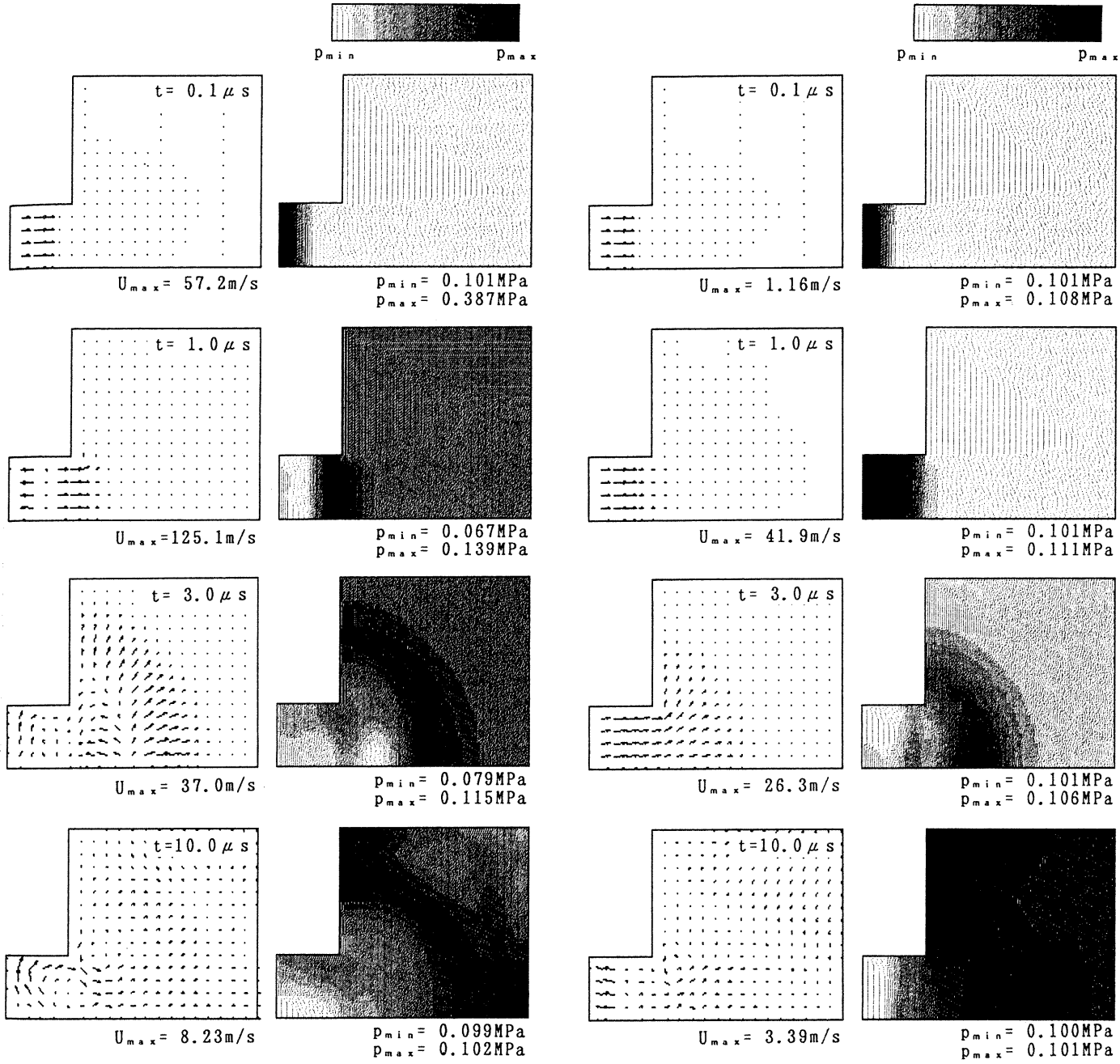

(a) In the case of capasitive discharge

(b) In the case of inductive discharge

Fig. 3 Computed flow and pressure fields in early stages of capacitive and inductive discharges.

The Formation of flow and thermal field by Capacitive/Inductive Discharge

First, the effect of a capacitive or a inductive discharge on the formation of flow and thermal fields is evaluated by observing the results of type A and type B.

Figures 3(a) and 3(b) show the early process of formation of flow field comparing the capacitive discharge(type A) with the inductive discharge(type B). In these figures, the flow fields and the pressure fields inside a solid line in Fig. 1 are represented as vector expressions and as gray level expressions, respectively. As shown in Fig. 3, when the time is 0.1 microseconds after the beginning of discharge, the high pressure region is formed near the center axis, and the radial flow toward outside is generated in both discharges of capacitive and inductive discharge. However, there are large differences in maximum pressure and in maximum velocity between capacitive and inductive discharges. The maximum pressure in capacitive discharge reaches almost four times of atomospheric pressure and the maximum velocity is approximatly 57 m/s, but the increasing ratio from the atomospheric pressure in the inductive discharge is less than 10 % and the maximum velocity is

approximatly 1.2 m/s. When the time is 1 microsecond through 3 microsecconds after the beginning of discharge, it is shown that reflux toward the gap is formed in the capacitive discharge because of reduced pressure region in the gap due to the propagation of pressure wave. In the inductive discharge in which the discharge is maintained in these periods, there is small difference between the pressure in the gap and pressure wave, so the reflux is not formed. At 10 microseconds after the beginning of discharge, the pressure wave has been propagated and a vortical convection is formed in the gap in case of capacitive discharge. In case of inductive discharge, however, the reflux is formed at this time, but the convection field is not yet formed.

The hot gas spots produced by these discharges stay near the center axis within 10 microseconds. The maximum temperature in the case of capacitive discharge is about 1200 K at 0.1 microseconds. The maximum temperature in the case of inductive discharge is about 2700 K at 10 microseconds, and is more than two times higher than that of capacitive discharge.

The growth of hot gas spot after the discharge and after the propagation of pressure wave is indicated in Figs4. (a) and 4(b). In the case of capacitive discharge shown in Fig. 4(a), the vortical convection field is already formed as mentioned above, then the hot gas spot is transported to the

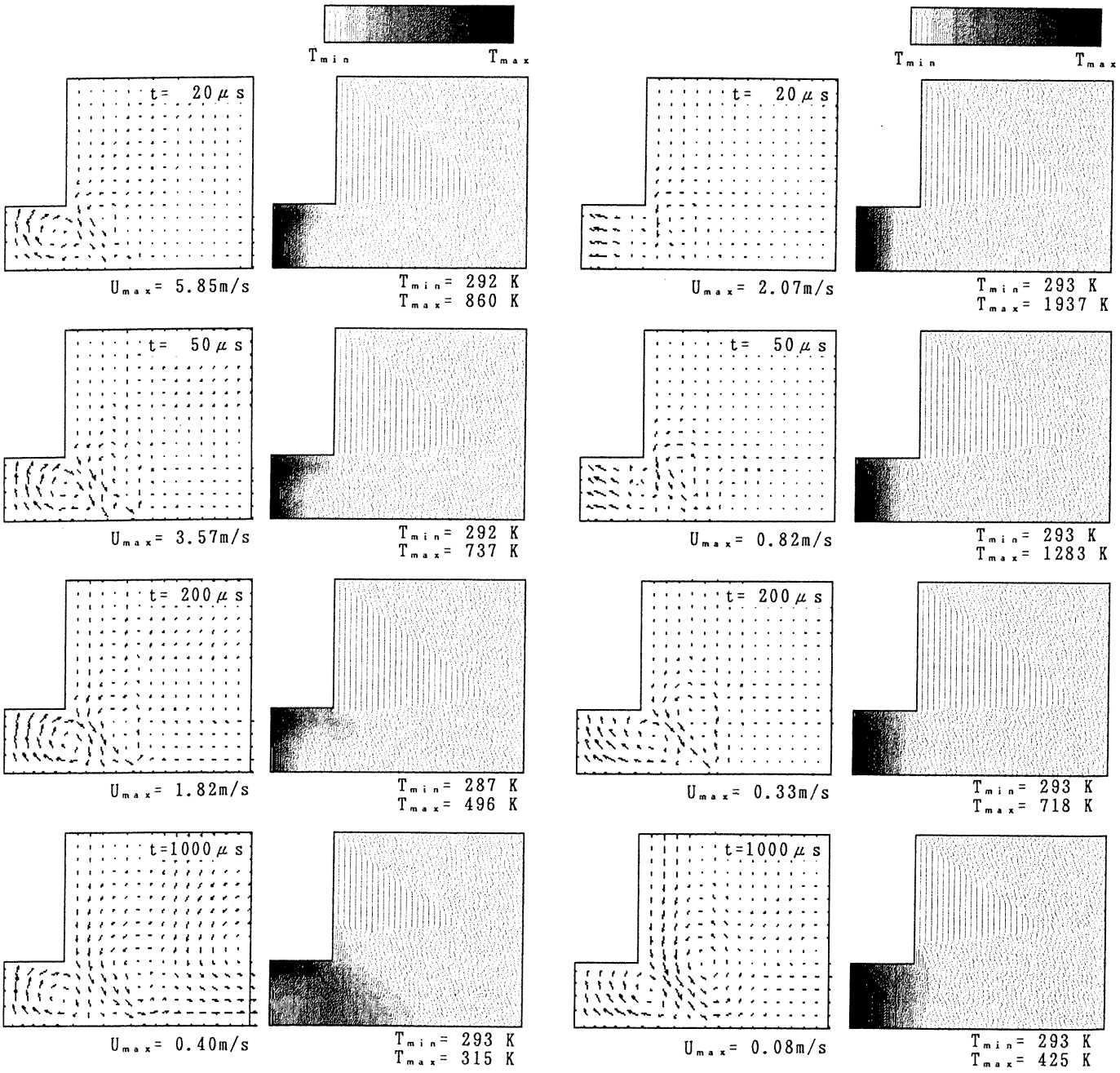

(a) In the case of capasitive discharge

(b) In the case of inductive discharge

Fig. 4 Computed flow and thermal fields after the propagation of pressure wave.

outside of gap through the vicinity of electrodes by the convection, but the maximum temperature at 1 milisecond is not so high. In the case of inductive discharge, the temperature of hot gas spot is high, but the formation of vortical convection is much slower than that in the case of capacitive discharge, and the convection velocity formed is very small. Then the growth of hot spot in the inductive discharge depends on the conduction process, and stays in the gap at 1milisecond after the beginning of discharge.

The Effects of Capacitive and Inductive Components on the Growth of Hot Gas Spots

The effects of capacitive component andinductive component in a composite discharge on the growth of hot gas spot was simulated using a condition of type C. The typical results are shown in Figs. 5(a),(b). Fig. 5(a) shows the early stage of flow and pressure fields, and figure 5(b) shows the growth of hot gas spot with the flow and thermal fields. As can be seen from Fig. 5(a) and Fig3(a), the formation of reflux in the composite discharge is almost the same as the capacitive discharge. Therefore, it is supposed that the capacitive component plays an important role in the formation of convection field. From Fig. 5(b), the temperature and volume of the hot gas spot in the composite discharge is much higher and larger than those in the capacitive discharge. It seems to be a contribution of the inductive component. In order to evaluate the detail, the time changes of maximum and minimum pressures in the composite discharge are compared with those in the capacitive discharge and with those in the inductive discharge. As shown in Fig. 6, the maximum pressure in both the composite discharge and the capacitive discharge rises rapidly just after the beginning of discharge, and the pressure in the gap is dropped under atomospheric pressure, and it is supposed that this large pressure difference causes the formation of convective motion. In the inductive discharge, the pressure rise is very small and the pressure drop is neglegible. Then it is not enough to form the convective motion. Moreover, the time changes of maximum velocity and maximum temperature in the composite discharge are compared with those in the capacitive discharge and with those in the inductive discharge, and are indicated in Fig. 7 and Fig. 8, respectively. In the case of composite discharges, the time change of maximum velocity is almost the same as that of capacitive discharge, and the maximum temperature converges to the maximum one of inductive discharge after 100 microseconds. These results indicate that the capacitive component contributes the formation of convection and the inductive component contributes the temperature rise.

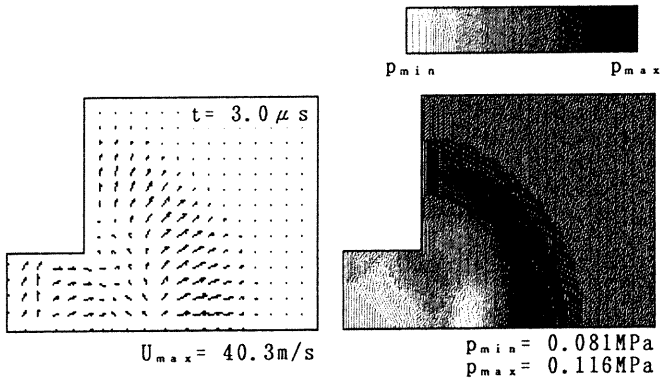

(a) Flow and pressure fields in early stage

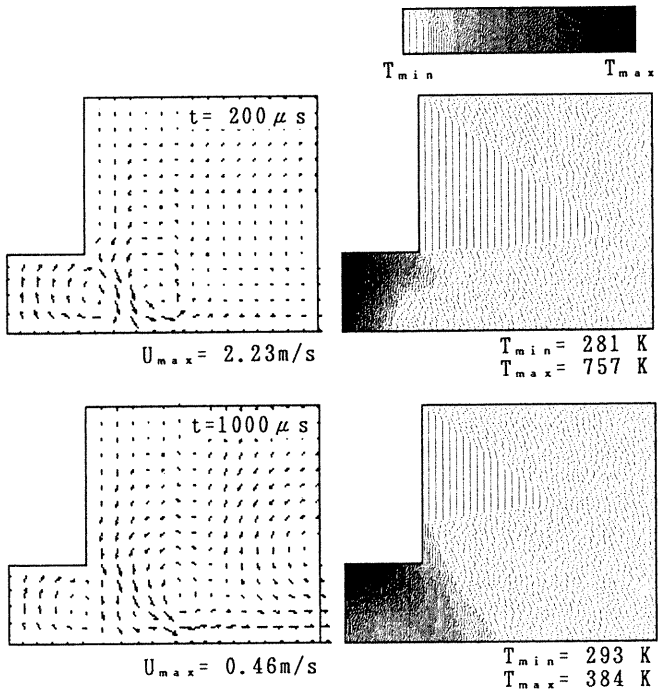

(b) Flow and thermal fields after the propagation of pressure wave

Fig. 5 Formation of flow field and growth of hot gas spot in composite discharges

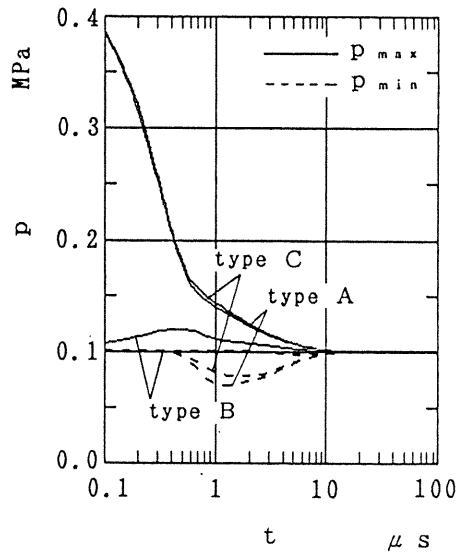

Fig. 6 Time changes of maximum and minimum pressure

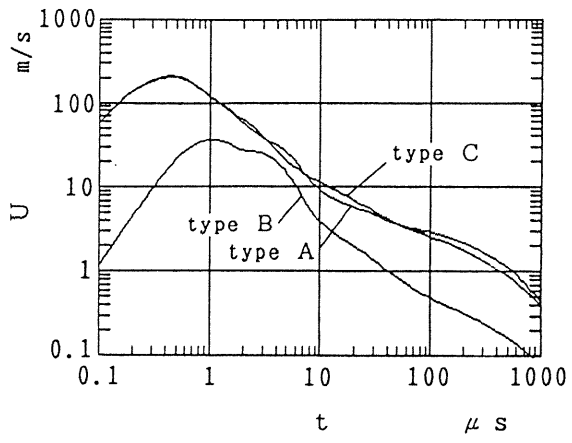

Fig. 7 Time changes of maximum velocity

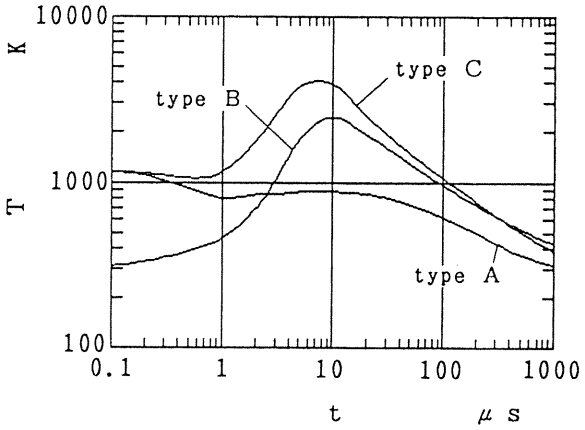

Fig. 8 Time changes of maximum temperature

CONCLUSIONS

From the results of numerical simulation, next facts with respect to the effect of capacitive and inductive components are revealed.

(1) In the case of capacitive discharge only, vortical convection is formed in a gap due to the strong pressure difference in early stage, and hot gas spots is transported by this vortical convection, but the temperature is not so high.

(2) In the case of inductive discharge only, the temperature of hot gas spots are considerably higher than that in the case of capacitive discharge, but the hot gas spots are not transported because of the weak convection field.

(3) In the case of composite discharges, the formation of convection field depends on the capacitive component and the temperature of hot gas spots depends on the inductive component.

NOMENCLATURE

De = diameter of electrode
Dp = diameter of heat generation area modeled as discharge plasma
e = total energy
p = pressure
Q = heat generation per unit volume
Qc = capacitive heat generation component per unit time
Qi = inductive heat generation component per unit time
q = heat flux
R = gas constant
r = radial coordinate
T = absolute temperature
t = time
U = velocity
u = radial velocity component
v = axial velocity component
z = axial coordinate
γ = ratio of specific heates
κ = thermal conductivity
λ = coefficient of bulk viscosity
μ = coefficient of molecular viscosity
ρ = fluid density
τ_{ij} = viscous shear stress tensor

Subscripts
max= maximum value
min= minimum value
r = radial direction
z = axial direction
θ = angular direction
∞ = pseudo-far-field boundary

REFERENCES

1. Ballal, D. R. and Lefebvre, A. H., "The Influence of Spark Discharge Characteristics on Minimum Ignition Energy in Flowing Gases," Combustion and Flame, Vol. 24, pp. 99-108, 1975.
2. Ziegler, G. F. W., Wagner, E. P. and Maly, R. R., "Ignition of Lean Methane-Air Mixtures by High Pressure Glow and Arc Discharge," 20th Symposium(International) on Combustion, The Combustion Institute, pp. 1817-1824, 1984.
3. Kono, M., Hatori, K. and Iinuma, K., "Investigation on Ignition Ability of Composite Sparks in Flowing Mixtures," 20th Symposium (International) on Combustion, The Combustion Institute, 1984.
4. Witze, P. O., Hall, M. J. and Bennett, M. J., "Cycle-Resolved Measurements of Flame Kernel Growth and Motion correlated with Combustion Duration, "SAE Paper 900023, 1990.
5. Pischinger, S. and Heywood, J. B., "How Heat Losses to the Spark Plug Electrodes Affect Flame Kernel Development in an SI-Engine," SAE Paper 900021, 1990.
6. MacCormack, R. W., "The Effect of Viscosity in Hypervelocity Impact Cratering," AIAA Paper No. 69-354, 1969.